PREPRINT DRAFT COMPUTATIONAL NEUROSCIENCE SIMULATION STUDY 14 SEP 2026

Ripe or rotting: hunger, yeast and distance decide which banana a simulated fruit fly chooses

Charbel Kassab · charbel@kassab.org

Code and data: github.com/charbelkassab/ripe-or-rotting

Project: charbelk.com/ripe-or-rotting

A connectome-constrained simulation of *Drosophila melanogaster* foraging, from fermentation chemistry and odour plume physics to receptor transduction, whole-nervous-system activity and flight.

ABSTRACT

Fruit flies are famously drawn to fermenting fruit, but it is unclear whether that preference reflects a stronger odour, a better taste, or the fly's internal state. We built an end-to-end simulation that computes banana composition over 14 days from ripening and yeast fermentation kinetics, the emission and turbulent transport of eleven volatiles and CO_2, receptor responses from measured odorant–receptor and taste data, and the resulting activity of the full male central nervous system connectome (MaleCNS v1.0; 165,122 neurons) in four internal states. Flies then searched a turbulent plume with a surge-and-cast flight rule and decided whether to feed from the brain's taste response.

Fermentation lowered the brain's odour detection threshold about tenfold and extended detection range roughly threefold (about 8–19 m vs 2–6 m in a 0.3 m/s breeze). Starvation doubled the range for ripe banana, so from 10 m fed flies landed first on rotting fruit (62–70%) while starved flies chose evenly. Within a few metres, smell intensity did not decide which fruit was reached. On contact, rotting pulp was less acceptable than ripe pulp, but surface yeast reversed this, most strongly in protein-deprived flies. The model reproduced four of nine behavioural and physiological checks; it failed to predict odour valence, lateralised steering and the effect of hunger on upwind flight.

1 Introduction

Wild *Drosophila melanogaster* feed and breed on fermenting fruit. Yeast-colonised substrates attract more flies than sterile fruit[1], fermentation volatiles such as ethanol, acetic acid and 2-phenylethanol act together as attractants[2], and yeast is the fly's main source of protein[3]. Three explanations for the preference are usually conflated: fermenting fruit is *louder* (it emits more volatiles), it *tastes* better (yeast and its products are appetitive), or the fly's *need* (energy vs protein) changes how both are valued[4,5].

A connectome now exists for the entire adult male central nervous system[6], and leaky integrate-and-fire (LIF) models of fly connectomes can predict sensorimotor circuit activity[7]. We asked whether a simulation that starts from the chemistry of real fruit, rather than from abstract "sweet" or "yeasty" stimuli, can separate these explanations, and where such a model breaks.

2 Methods

The simulation is a chain of six stages, each driven by measured parameters wherever they exist. Parameters without direct measurements are flagged as estimates in the source files and in the text below.

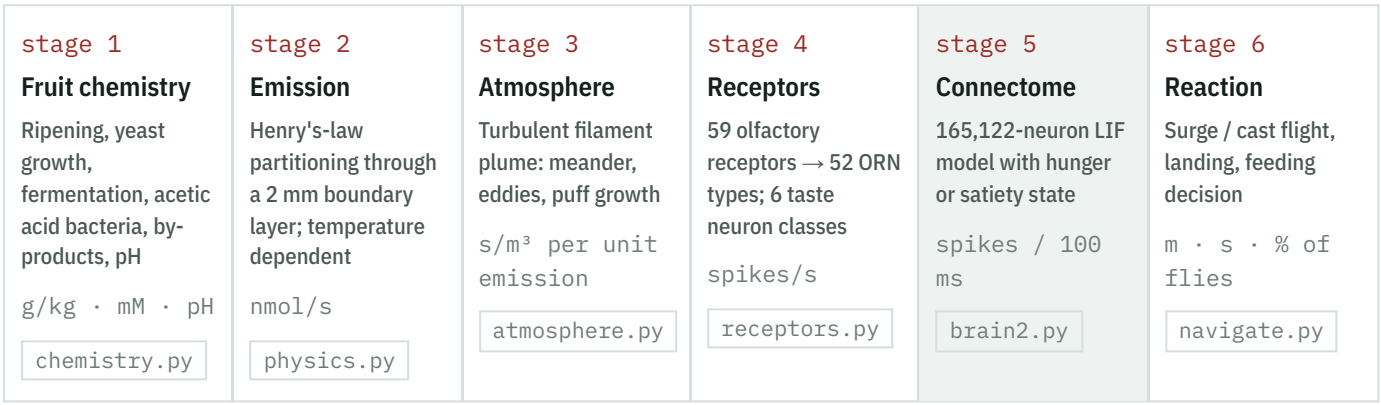

Figure 1. Simulation pipeline. Stage 5 is the only stage built from the connectome; stages 1–4 are physical and physiological models, and stage 6 combines brain outputs with measured flight behaviour.

2.1 Fruit chemistry

Pulp starts at eating-ripe composition (Cavendish: starch 25.2, sucrose 45.6, glucose 53.3, fructose 62.3 g/kg; water 753 g/kg)[8]. Starch hydrolysis and invertase continue ripening in both scenarios. In the *damaged* scenario, yeast (10^5 CFU/g inoculum; μ_{max} 0.22 h^{-1} at 25 °C, K_s 0.1 g/L, $Y_{x/s}$ 0.10)[9] converts hexose to ethanol and CO_2 (0.46 g ethanol per g sugar). Acetic acid bacteria oxidise ethanol at the surface (53% of theoretical yield, as measured for banana vinegar). By-products (ethyl acetate, acetoin, 2-phenylethanol, isoamyl alcohol, glycerol) use wine-fermentation yields. pH comes from a weak-acid charge balance on malic, citric and acetic acid and dissolved CO_2, calibrated to pH 4.9 for ripe pulp. Fruit-made esters and aldehydes are interpolated between ripe and overripe estimates. Biological rates scale with $Q_{10} = 2$.

2.2 Emission and atmosphere

Each volatile leaves 30 cm^2 of exposed pulp (an estimate for a split banana) at $J = (D/\delta) \cdot A \cdot K_{aw}(T) \cdot C_{aq}$, using measured air diffusion coefficients and Henry's-law constants with their temperature dependence[10,11]; only undissociated acetic acid partitions to air. CO_2 combines fruit respiration (200 µL/min)[12] with fermentation (272 mL per g sugar).

Transport uses a filament model[13]: 25 puffs/s per source, a spatially uniform crosswind meander (Ornstein–Uhlenbeck, s.d. 0.5 U, τ 2 s), per-puff eddy velocities (s.d. 0.33 U, τ 0.2 s) and linear puff growth. Parameters were chosen so that, 0.1–2 m downwind, intermittency is 0.30–0.41, 95th-percentile concentration is 5.5–7× the mean, and the mean is within a factor of three of a Gaussian plume ($\sigma = 0.1$ r). Beyond 2 m this plume stays up to 3× more concentrated than the Gaussian estimate, so far-field experiments were repeated with faster puff growth that dilutes as expected.

2.3 Receptor transduction

Olfactory receptor responses are DoOR 2.0 consensus values[14] (spontaneous rate subtracted) scaled to a 290 spikes/s maximum[15], with a population Hill slope of 0.8[16] around the concentration used in the underlying recordings. Receptors map to connectome ORN types through their glomeruli (VC3/VC5/VM6 renaming applied). CO_2 drives the V glomerulus above a ~1,000 ppm excess. Spontaneous ORN firing is 8 spikes/s.

Taste neuron identities in the male connectome were assigned by matching each labellar type's downstream connectivity to FlyWire neurons of known modality[7,17] (cosine similarity 0.83–0.94): LB3b–d sugar, LB3a water, LB1a–d bitter, LB1e Ir94e, dorsal taste pegs amino acid/yeast, claw taste pegs carbonation[18]. Sugar neurons follow a sucrose Hill curve (EC_{50} 60 mM, max 94 spikes/s) with weaker glucose and fructose responses; water neurons are silenced by osmolality; bitter neurons respond to tannins and K^+ (thresholded), ethanol and acidity; yeast-peg neurons respond to yeast (EC_{50} 2% w/v, estimate)[5,19]. Bitter input suppresses sugar-neuron output, `sugar / (1 + bitter / 15 Hz)`, standing in for presynaptic GABA-B inhibition, which a point-neuron connectome model cannot represent[20].

2.4 Connectome model

The 165,122 traced neurons and 25.6 M connections of MaleCNS v1.0[6] were simulated as identical LIF units[7] (1 ms step, 2 ms delay, synapse sign from predicted transmitter). With published parameters this dataset locks into self-sustaining activity, so we applied: spike-frequency adaptation; synapse gain 0.2 mV per contact; inhibition ×3 (a stand-in for slow GABA-B); no fast synaptic action for dopamine, serotonin or octopamine; no Kenyon cell–Kenyon cell contacts; and sensory neurons treated as pure inputs. Odour responses were still identical for every receptor class (projection-neuron pattern correlation 0.98), because 30 cholinergic antennal-lobe local neurons (lLN1_bc) formed a recurrent loop. Reducing cholinergic local-neuron chemical output tenfold, since these cells act largely through gap junctions[21], made odour patterns distinct (correlation 0.00).

2.5 Internal states

Four states combine literature gains at the periphery with tonic drive (15 Hz) to the connectome's own state neurons. **Fed**: drive to insulin-producing cells and Hugin neurons. **Starved 24 h**: sugar-neuron sensitivity ×2 and bitter ×0.6[22]; DM1 ORN output ×1.75, DM2/DM4 ×1.3, VM2/VA3 ×0.8[23]; DM5 ×0.25[24]; drive to NPF neurons. **Protein-deprived**: yeast taste-peg gain ×1.5 (estimate after ref. 5). **Both**: the union. Hunger was first implemented as an output gain; that failed the held-out feeding test (Section 4), so sugar and bitter gains now scale effective concentration (sensitivity).

2.6 From brain activity to behaviour

Feeding. Acceptance is the spike count over 400 ms in the proboscis motor neuron MN9, the feeding neuron Fdg, G2N-1 and the sugar-responsive second-order neurons[7,25]; aversion is the spike count in MDN and Bitter-SEL. The feeding probability on landing was calibrated so that fed flies accept 800 mM sucrose 55% of the time[22]. Because model acceptance saturates above ~300 mM, this logistic is steep; a saturating alternative, $p = A / (A + A_{800})$, is reported alongside it.

Odour detection. For each food and state, the whole brain was run for 100 ms at 13 plume concentrations (four repeats), and a detection was scored when projection-neuron spikes exceeded the no-odour baseline by three standard deviations. The navigation model looks up this detection probability at each fly's instantaneous plume concentration every 50 ms.

Flight. Flies surge upwind 190 ± 75 ms after a detection and cast crosswind 450 ± 165 ms after losing the odour[26], with widening reversals. Within 15 cm a surging fly flies to the visible fruit (odour-gated visual attraction)[27]. Flies that reject a fruit take off and ignore it for 5 s. These rules come from behaviour, not from the connectome, because the model did not steer (Section 3.3). An optional valence gate lets flies surge only if the evoked projection-neuron pattern is net attractive under literature glomerular valence[28,29], counting CO_2 as attractive in flight[30].

2.7 Experiments

Two fruits sat 30 cm apart, 0.3 m/s wind, 25 °C, with 120 flies released 2 m downwind per run. Each of eight plume realisations was run in both fruit orientations, because a single realisation's meander can favour one side for tens of seconds (a same-fruit control split 66/34 before this correction and 50/50 after it). The spread across realisations is reported as s.d. Additional runs varied release distance (1–15 m), fruit separation (0.3–4 m), wind (0.15–0.6 m/s) and temperature (18–32 °C).

3 Results

3.1 Fermentation turns a banana into a different chemical object

Intact fruit kept ripening: sugars rose from 1,029 to ~1,320 mM in tissue water and pH stayed at 4.9. Seven days after colonisation, damaged fruit held 2.0% ethanol, 0.25% acetic acid, 1.5 g/kg dry yeast and 94 mg/kg ethyl acetate, with sugars down to 909 mM and pH 4.31. By 14 days it reached 3.0% ethanol and 0.8% acetic acid, within the 1–4.5% ethanol measured in naturally fermenting fruit[31]. Emission changed far more than composition: ethyl acetate rose ~180× (0.68 to 123 nmol/s) and ethanol ~64× (35 to 2,270 nmol/s), while the fruit's own esters changed less than twofold. Warmth amplified fermentation: at day 7, ethyl acetate emission was 54, 123 and 279 nmol/s at 18, 25 and 32 °C.

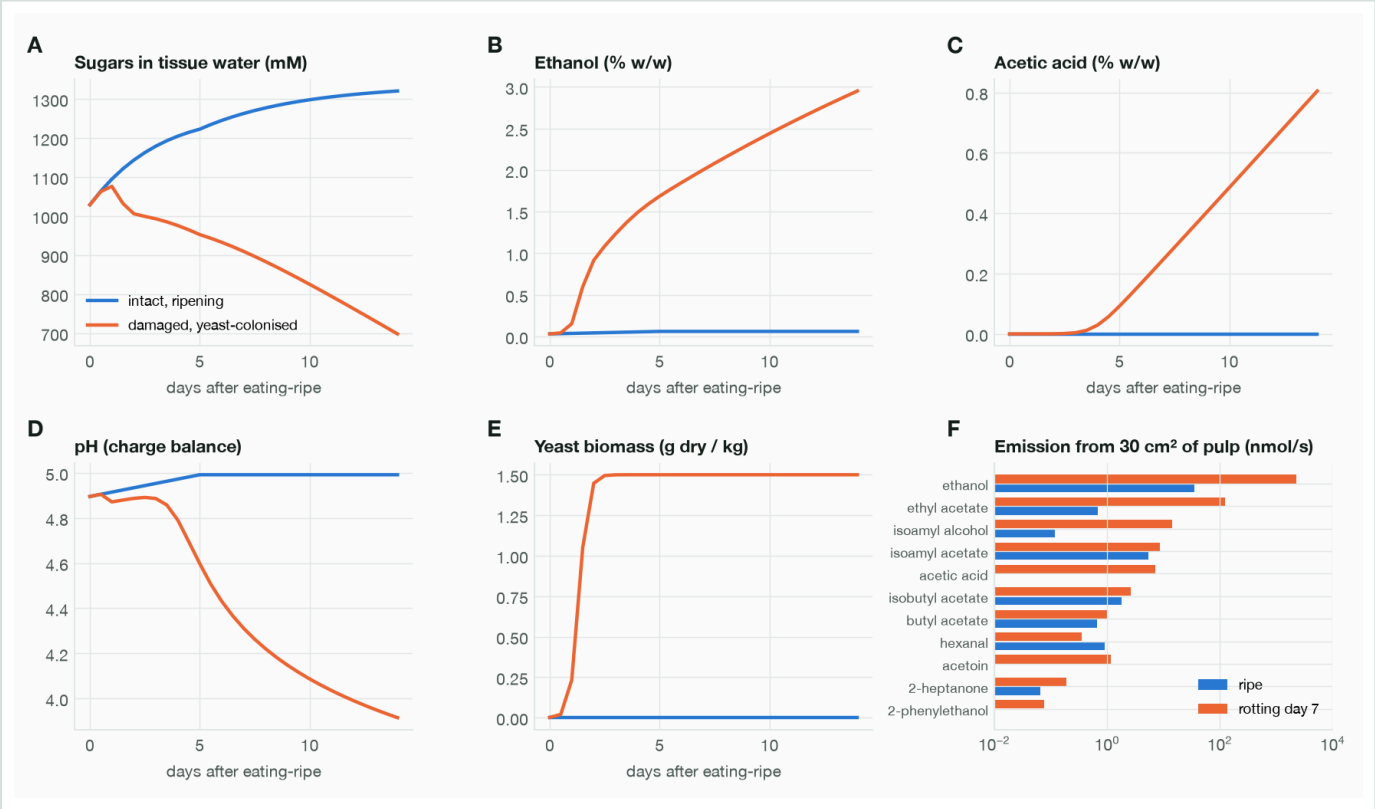

Figure 2. Banana composition from kinetics. **A–E** Intact (blue) vs yeast-colonised (orange) pulp. **F** Volatile emission from 30 cm² of pulp, ripe (day 0) vs rotting (day 7), log scale.

3.2 The odour a fly meets is intermittent

At any point in the plume, odour was absent most of the time and arrived as brief filaments up to 16–24× the mean (Fig. 3A–C). Within 2.8 m the brain detected either fruit with similar probability, because filaments exceeded both detection thresholds; intermittency, not concentration, limited detection at close range.

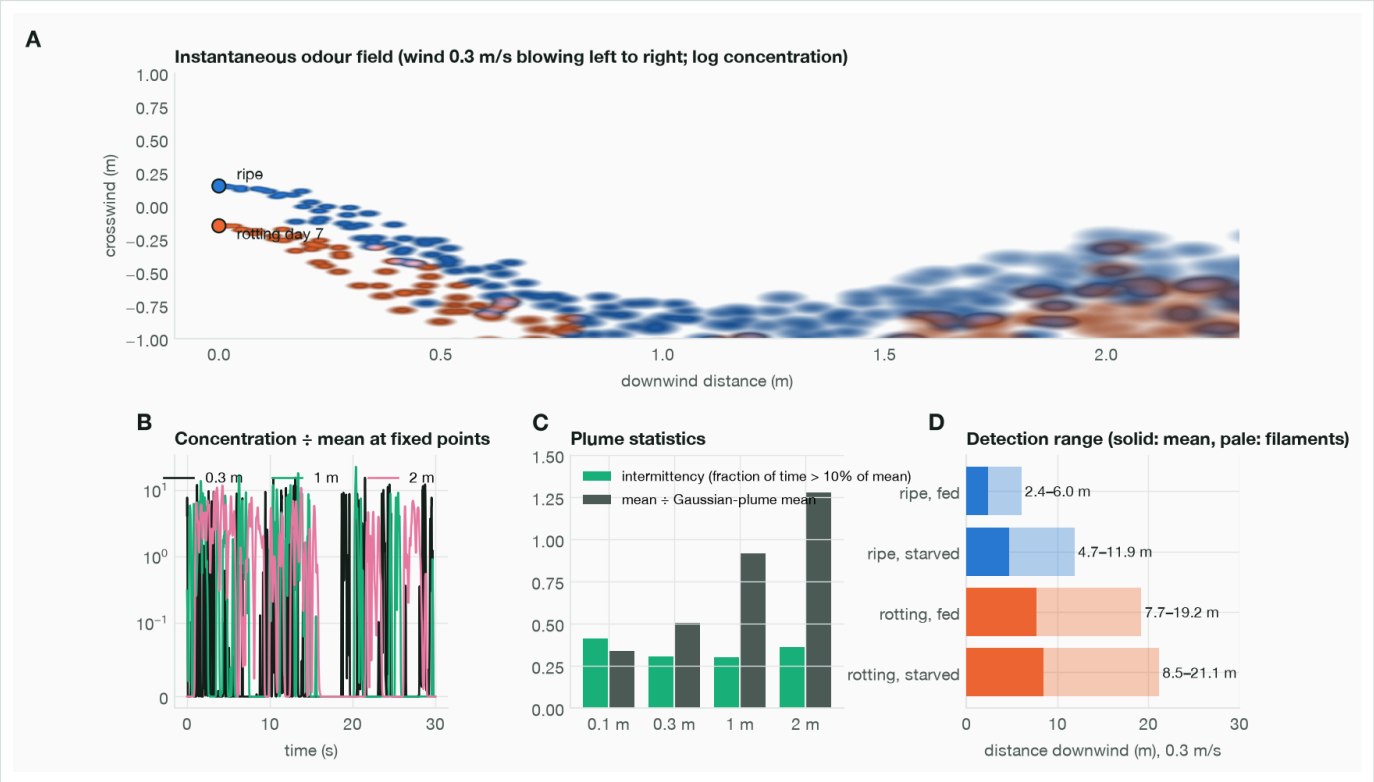

Figure 3. Atmosphere. **A** Instantaneous filament field from ripe (blue) and rotting (orange) fruit. **B** Concentration relative to its mean at 0.3, 1 and 2 m. **C** Intermittency and ratio to a Gaussian plume. **D** Distance at which the plume's mean (solid) or 95th-percentile filament concentration (pale) reaches the brain's 50% detection threshold (0.3 m/s, σ = 0.1 r).

3.3 The connectome detects fermentation at a tenth of the concentration, but does not steer

Projection-neuron responses rose smoothly with concentration (Fig. 4A). The 50% detection threshold was 17.8 s/m^3 for ripe banana and 1.78 s/m^3 for rotting banana in fed flies, a tenfold difference driven by ethyl acetate, isoamyl alcohol and the esters of fermentation. Starvation lowered the ripe threshold fourfold (to 4.6 s/m^3), mainly through DM1 and DM2 facilitation, and barely changed the rotting threshold (1.47 s/m^3). Warmth lowered thresholds through faster fermentation and higher volatility (rotting: 5.6, 1.8 and 1.0 s/m^3 at 18, 25 and 32 °C).

Activity reached projection neurons 4 ms, lateral horn neurons 6 ms and descending neurons 21 ms after ORN spiking began. Odour on one antenna did not lateralise output: the turning neurons DNa01/DNa02 stayed silent, and descending output was right-dominant whichever side was stimulated (index −0.88 to −0.93; Fig. 4C). This reflects the uneven side annotation of ORNs (1,343 right, 883 left, 409 unassigned) as much as any circuit property, and it is why the flight rule uses behavioural parameters instead of brain steering.

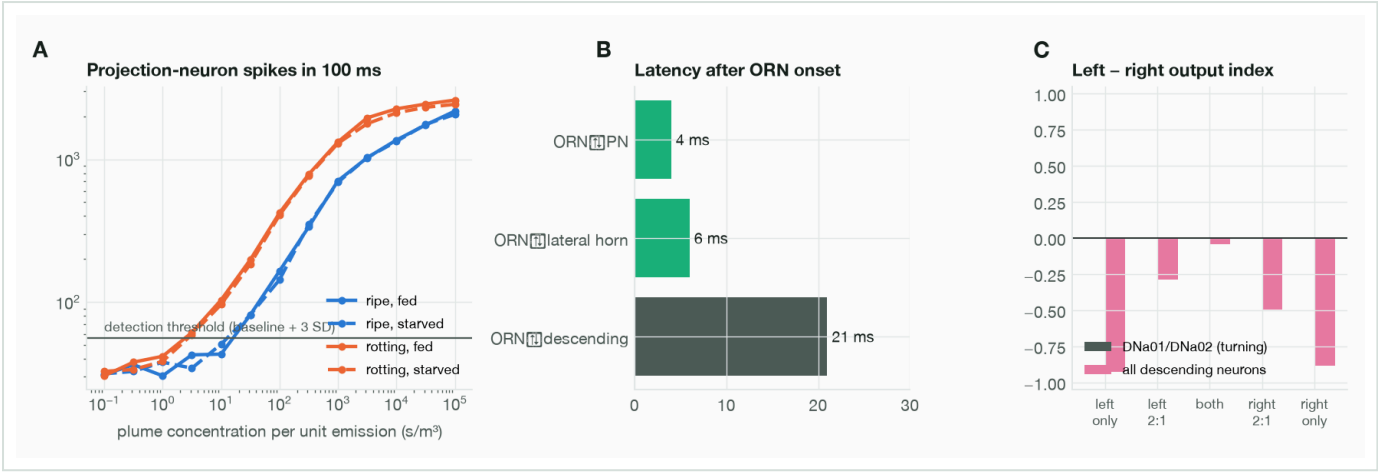

Figure 4. Whole-brain olfactory response. **A** Projection-neuron spikes per 100 ms vs plume concentration per unit emission, including spontaneous ORN firing; horizontal line: detection threshold. **B** Onset latency. **C** Left – right output index for unilateral and bilateral stimulation; turning neurons were silent in all conditions.

3.4 Rotting banana is visible to the brain from about three times farther

Combining thresholds with plume dilution (Fig. 3D), a fed fly downwind of ripe banana first detected it 2.4 m (mean plume) to 6.0 m (filaments) away; for rotting banana the range was 7.7–19.2 m. Starvation extended the ripe range to 4.7–11.9 m. The rotting range grew from 4.3–10.8 m at 18 °C to 10.3–25.6 m at 32 °C. In a 1 m/s wind every range roughly halved.

3.5 On contact, pulp favours ripe fruit and surface yeast favours rotting fruit

Ripe pulp drove sugar neurons at 57 spikes/s with little bitter input (5.8). Rotting pulp at day 7 drove them at only 27, because of less sugar, acid suppression and 24 spikes/s of bitter input from acidity and ethanol. Averaged through the fruit, rotting pulp was 2–4× less acceptable than ripe pulp in every state (Table 1). Where yeast grows on the surface (×20 local yeast, an estimate), taste pegs fired at 55 spikes/s and rotting fruit became as acceptable as ripe for fed and starved flies, and clearly more acceptable for protein-deprived flies (9.8 vs 6.2 spikes; 13.2 vs 8.3 when also starved).

Table 1. Feeding-neuron spikes in 400 ms (mean of 6 simulations)

Food	Fed	Starved 24 h	Protein-deprived	Both
Ripe, day 0	6.3	9.0	6.2	8.3
Overripe, day 5	6.8	8.7	7.2	8.5
Rotting day 2, pulp	3.5	5.2	2.8	4.7
Rotting day 7, pulp	1.8	3.2	2.2	2.8
Rotting day 2, surface yeast	9.3	11.3	13.0	17.5
Rotting day 7, surface yeast	7.3	8.0	9.8	13.2
Rotting day 14, surface yeast	6.2	7.5	10.8	9.5

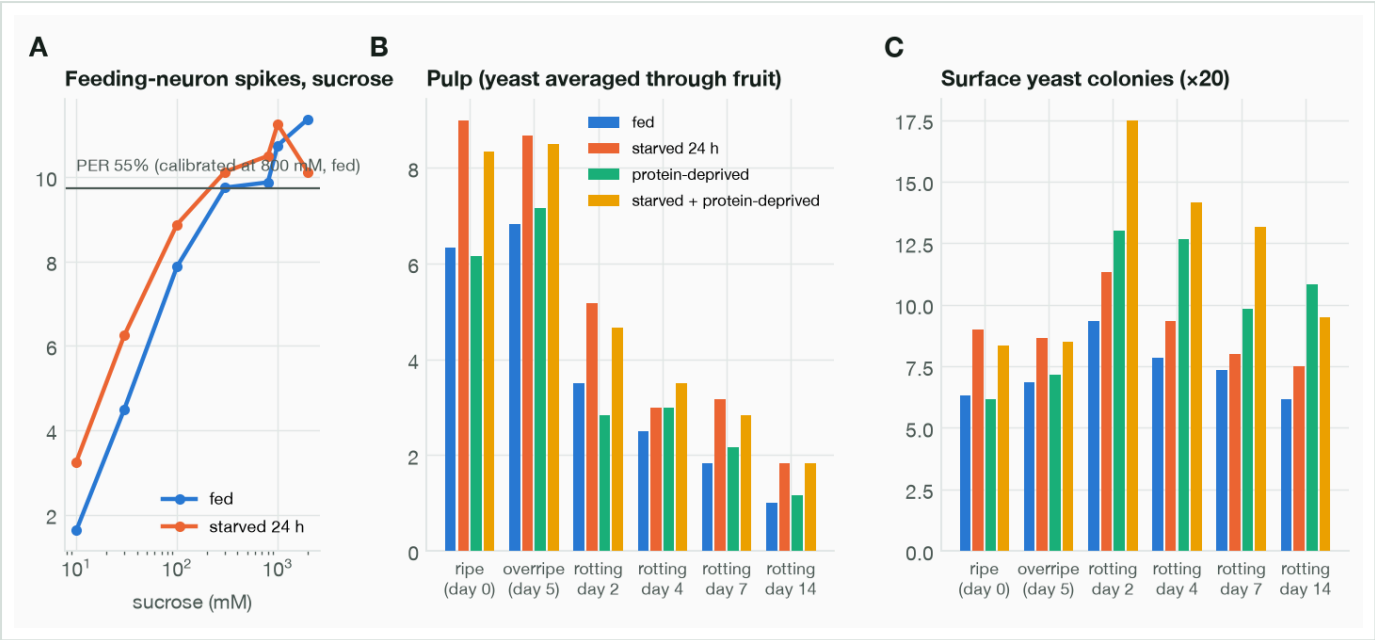

Figure 5. Taste. **A** Feeding-neuron response to sucrose; horizontal line: 55% proboscis extension, calibrated on fed flies at 800 mM[22]. **B** Pulp. **C** Surface yeast colonies (rotting fruit only; ripe and overripe repeated for comparison).

3.6 Within a few metres, flies reach whichever fruit the plume brings them to

With a single fruit, 57–62% of flies landed within 90 s regardless of food or state, but feeding depended strongly on both: 0.5% of fed and 31% of starved flies fed on ripe banana, and 6% of fed and 14% of starved flies on rotting banana. In the two-choice arena, first landings split evenly (50–53% on rotting, s.d. across plumes 3–5%) in every state, at every release distance from 1 to 15 m in the baseline plume, at all three wind speeds and at all three temperatures.

Feeding did not split evenly. With surface yeast, protein-deprived flies fed mostly on rotting fruit (99% under the calibrated decision rule, 60% under the saturating rule), while sugar-starved flies were the least drawn to it (30% and 52%). Without surface yeast, all four states fed mostly on ripe fruit under both rules (43–46% rotting under the saturating rule; almost no rotting feeding under the calibrated rule). With the valence gate, fed and protein-deprived flies landed on rotting fruit first 78–80% of the time, but 27–28% never landed: under the literature valence code, ripe-banana odour scores as aversive at every concentration for non-starved flies, whereas dilute rotting-banana odour scores as attractive.

Movie 1 (still frame). Sixty flies deprived of food and protein search the two plumes. Grey: casting; green: surging after brain-detected odour; yellow: feeding. Full video: `paper/foraging.mp4`.

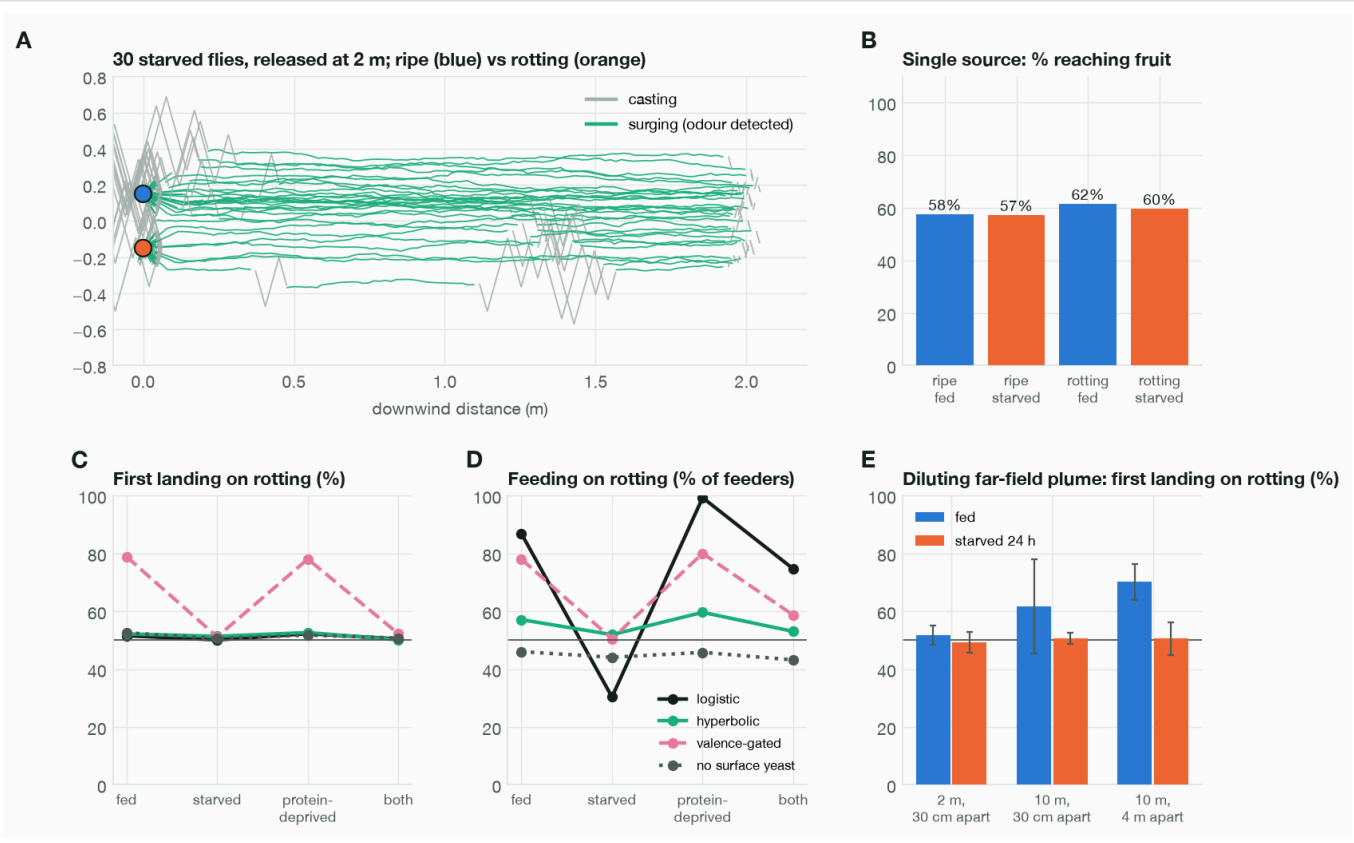

Figure 6. Stimulus → reaction. **A** Trajectories of 30 starved flies. **B** Single source: flies reaching the fruit within 90 s. **C** First landing on rotting fruit and **D** share of feeding on rotting fruit, by state, for four model variants. **E** Far-field test with a plume that dilutes as expected: first landing on rotting fruit (error bars: s.d. across plume realisations).

3.7 Beyond the ripe fruit's detection range, hunger removes the bias toward fermentation

Because the baseline plume stays too concentrated beyond 2 m, the long-range experiment was repeated with a plume that dilutes as expected (Fig. 6E). Released 2 m away, fed and starved flies still split evenly. Released 10 m away, beyond a fed fly's range for ripe banana, fed flies landed first on rotting fruit 62% (fruits 30 cm apart) and 70% (4 m apart) of the time. Starved flies, whose ripe-banana range extends past 10 m, split evenly (51%). This state effect appears only under the diluting plume, so its size depends on far-field turbulence, which we did not measure.

4 Validation

Each check compares a model output with an independent measurement or with a property the model must have. Calibration targets are marked as such and are not counted as validation.

Table 2. Checks against data

Check	Model	Reference	Result
Feeding neurons rise with sucrose concentration	`1.6 → 11.4 spikes, 10–2,000 mM`	Monotonic dose–response[22]	`pass`
Starvation increases acceptance	`4.0 → 5.8 at 30 mM`	Increased sugar sensitivity[22]	`pass`
Half-maximal proboscis extension, starved 1 day (held out)	`238 mM`	`300 mM`[22]	`pass`
Bitter suppresses sugar acceptance	`7.5 → 1.8`	Presynaptic inhibition[20]	`by construction`
Distinct odours give distinct projection-neuron patterns	`r = 0.98 → 0.00 after fix`	Glomerular coding	`pass`
Plume near-field statistics (0.1–2 m)	`intermittency 0.30–0.41`	Filament model[13]	`calibrated; far field too concentrated`
Odour attraction for 108 odorants (cross-validated)	`r = 0.06`	Trap attraction indices[28]	`fail`
Unilateral odour lateralises steering output	`DNa01/02 silent`	Flies turn toward the stronger antenna[32]	`fail`
Starvation increases upwind success to a food odour	`60% vs 62%`	`62% vs <20%`[33]	`fail`

The odour valence failure is not specific to the brain: a readout trained directly on receptor rates did no better (r = 0.09), so single-concentration receptor profiles alone may not predict trap attraction. The upwind-flight failure shows that hunger's effect on search behaviour is not captured by sensory gains alone.

5 Conclusions about fruit flies

Read these as predictions of a model that passed four of its nine checks, not as established facts. Each is testable.

1 Fermentation mainly makes fruit easier to detect.

Yeast volatiles lowered the brain's detection threshold tenfold and extended detection range about threefold, from metres to tens of metres in a light breeze, and further in warm weather.

`17.8 vs 1.78 s/m³ · 2.4–6.0 vs 7.7–19.2 m · rotting 4.3–10.8 m at 18 °C, 10.3–25.6 m at 32 °C`

2 The long-range pull of rotting fruit should be strongest in fed flies.

Starvation sensitises the receptors that ripe fruit engages, closing the detection gap; from 10 m, fed flies chose rotting fruit first and starved flies did not.

`fed 62–70% · starved 51% · diluting far-field plume only`

3 Up close, odour intensity does not choose between fruits.

Within a few metres both plumes exceed detection thresholds in every filament, and which fruit a fly reaches depends on the plume's path and on vision at landing.

`50–53% first landings on rotting fruit across states, 1–15 m (baseline plume), wind and temperature`

4 Rotting fruit tastes worse; the yeast on it tastes better.

Fermentation removes sugar and adds acid and ethanol, which suppress sugar neurons. Surface yeast colonies more than compensate, so the attractive part of rotting fruit is the yeast, not the rot.

`pulp: rotting 2–4× less acceptable · surface yeast: equal or higher`

5 What a fly eats depends on what it lacks.

Protein-deprived flies should feed on yeasty fruit; sugar-starved flies should be the least drawn to it and remain willing to eat fresh ripe fruit.

`feeding on rotting: protein-deprived 60–99% · sugar-starved 30–52%`

6 The attraction of fermenting fruit is two mechanisms, not one.

Far-reaching fermentation volatiles bias well-fed flies at a distance, and yeast taste biases protein-hungry flies on contact. Neither amounts to a general preference for rot.

Suggested experiment: release fed and 24 h-starved flies 10 m downwind of paired ripe and yeast-inoculated banana in a field tunnel, and score first landings separately from feeding with antennae-intact vs olfaction-deficient (Orco) flies and protein-deprived groups. The model predicts a state × distance interaction for landing and a protein-state effect for feeding.

---

6 Limitations

Connectome model. Every neuron is the same point unit, synapse strength is synapse count × a constant, and six structural changes were needed to prevent runaway activity. The male connectome

cannot represent the mated female, whose yeast appetite is the strongest known[3,4]. Brain state is reset between decisions; there is no learning or post-ingestive feedback.

Chemistry. Per-compound banana volatile contents, rotting-fruit ethanol and acetic acid trajectories, the 30 cm^2 exposed area and the ×20 surface yeast enrichment are estimates. Temperature affected smell but not the taste grid, which was computed at 25 °C.

Atmosphere. The plume is two-dimensional at fly height, meander is spatially uniform, and far-field dilution depends on an uncalibrated growth parameter that changes the long-range result.

Behaviour. Steering, surge and cast timing come from wind-tunnel data, not from the connectome. Hunger does not change flight behaviour itself. Bitter–sugar interaction is added outside the connectome, and the two feeding decision rules disagree for sugar-starved flies.

7 References

1. Becher PG et al. (2012) Yeast, not fruit volatiles mediate *Drosophila melanogaster* attraction, oviposition and development. *Funct Ecol* 26:822.
2. Zhu J, Park KC, Baker TC (2003) Identification of odors from overripe mango that attract vinegar flies. *J Chem Ecol* 29:899.
3. Ribeiro C, Dickson BJ (2010) Sex peptide receptor and neuronal TOR/S6K signaling modulate nutrient balancing in *Drosophila*. *Curr Biol* 20:1000.
4. Corrales-Carvajal VM, Faisal AA, Ribeiro C (2016) Internal states drive nutrient homeostasis by modulating exploration-exploitation trade-off. *eLife* 5:e19920.
5. Steck K et al. (2018) Internal amino acid state modulates yeast taste neurons to support protein homeostasis in *Drosophila*. *eLife* 7:e31625.
6. Google Research & HHMI Janelia FlyEM (2026) MaleCNS v1.0: connectome of the adult male *Drosophila* central nervous system. *Cell*; data male-cns.janelia.org, CC-BY 4.0.
7. Shiu PK et al. (2024) A *Drosophila* computational brain model reveals sensorimotor processing. *Nature* 634:210.
8. Phillips KM et al. (2021) Sugar and starch composition of bananas by ripeness stage. *PLoS ONE* 16:e0253366.
9. Verduyn C et al. (1990) Physiology of *Saccharomyces cerevisiae* in anaerobic glucose-limited chemostat cultures. *J Gen Microbiol* 136:395.
10. Sander R (2023) Compilation of Henry's law constants (version 5.0.0) for water as solvent. *Atmos Chem Phys* 23:10901.
11. Tang MJ et al. (2015) Compilation and evaluation of gas phase diffusion coefficients of reactive trace gases. *Atmos Chem Phys* 15:5585.
12. Faucher C et al. (2006) Behavioral responses of *Drosophila* to biogenic levels of carbon dioxide depend on life-stage, sex and olfactory context. *J Exp Biol* 209:2739.
13. Farrell JA, Murlis J, Long X, Li W, Cardé RT (2002) Filament-based atmospheric dispersion model to achieve short time-scale structure of odor plumes. *Environ Fluid Mech* 2:143.
14. Münch D, Galizia CG (2016) DoOR 2.0: comprehensive mapping of *Drosophila melanogaster* odorant responses. *Sci Rep* 6:21841.
15. Olsen SR, Bhandawat V, Wilson RI (2010) Divisive normalization in olfactory population codes. *Neuron* 66:287.
16. Si G et al. (2019) Structured odorant response patterns across a complete olfactory receptor neuron population. *Neuron* 101:950.
17. Schlegel P et al. (2024) Whole-brain annotation and multi-connectome cell typing of *Drosophila*. *Nature* 634:139.
18. Fischler W, Kong P, Marella S, Scott K (2007) The detection of carbonation by the *Drosophila* gustatory system. *Nature* 448:1054.

9. Cameron P, Hiroi M, Ngai J, Scott K (2010) The molecular basis for water taste in *Drosophila*. *Nature* 465:91.
10. Chu B, Chui V, Mann K, Gordon MD (2014) Presynaptic gain control drives sweet and bitter taste integration in *Drosophila*. *Curr Biol* 24:1978.
11. Yaksi E, Wilson RI (2010) Electrical coupling between olfactory glomeruli. *Neuron* 67:1034.
12. Inagaki HK, Panse KM, Anderson DJ (2014) Independent, reciprocal neuromodulatory control of sweet and bitter taste sensitivity during starvation in *Drosophila*. *Neuron* 84:806.
13. Root CM, Ko KI, Jafari A, Wang JW (2011) Presynaptic facilitation by neuropeptide signaling mediates odor-driven food search. *Cell* 145:133.
14. Ko KI et al. (2015) Starvation promotes concerted modulation of appetitive olfactory behavior via parallel neuromodulatory circuits. *eLife* 4:e08298.
15. Yao Z, Scott K (2022) Serotonergic neurons translate taste detection into internal nutrient regulation. *Neuron* 110:1036.
16. van Breugel F, Dickinson MH (2014) Plume-tracking behavior of flying *Drosophila* emerges from a set of distinct sensory-motor reflexes. *Curr Biol* 24:274.
17. Frye MA, Tarsitano M, Dickinson MH (2003) Odor localization requires visual feedback during free flight in *Drosophila melanogaster*. *J Exp Biol* 206:843.
18. Knaden M, Strutz A, Ahsan J, Sachse S, Hansson BS (2012) Spatial representation of odorant valence in an insect brain. *Cell Rep* 1:392.
19. Semmelhack JL, Wang JW (2009) Select *Drosophila* glomeruli mediate innate olfactory attraction and aversion. *Nature* 459:218.
20. van Breugel F, Huda A, Dickinson MH (2018) Distinct activity-gated pathways mediate attraction and aversion to CO_2 in *Drosophila*. *Nature* 564:420.
21. Dudley R (2004) Ethanol, fruit ripening, and the historical origins of human alcoholism in primate frugivory. *Integr Comp Biol* 44:315.
22. Gaudry Q, Hong EJ, Kain J, de Bivort BL, Wilson RI (2013) Asymmetric neurotransmitter release enables rapid odour lateralization in *Drosophila*. *Nature* 493:424.
23. Becher PG, Bengtsson M, Hansson BS, Witzgall P (2010) Flying the fly: long-range flight behavior of *Drosophila melanogaster* to attractive odors. *J Chem Ecol* 36:599.

Simulation code, parameter sources and raw results: github.com/charbelkassab/ripe-or-rotting (research/*.json cite every parameter; results/*.json hold every number in this paper).